Journal of Sound and Vibration (1997) **208**(5), 705–728

FORMULAS FOR MODAL DENSITY AND FOR INPUT POWER FROM MECHANICAL AND FLUID POINT SOURCES IN FLUID FILLED PIPES

S. FINNVEDEN*

Institute of Sound and Vibration Research, University of Southampton, Southampton, SO17 1BJ, England

(*Received* 1 *October* 1996, *and in final form* 27 *August* 1997)

Simple expressions for the modal density of fluid filled pipes and for the input power from mechanical and fluid point sources are derived. The derivations are based on a previously reported, simplified theory for the radial–axial motion of fluid filled pipes. These equations are recapitulated and criteria for their application are given. The accuracy of the resulting expressions for modal density and input power are verified with a spectral (frequency dependent) FE method. These FE calculations are based on the Arnold and Warburton theory for thin walled cylinder vibration and Helmholtz equation for fluid motion. The theory developed applies below half the ring-frequency and when higher order fluid modes are cut off. Thus, as an example, for a water filled steel pipe with a diameter of 300 mm, accurate predictions of modal density and input power are made for frequencies up to approximately 1 kHz.

1. INTRODUCTION

Vibrations in pipeworks often cause excessive noise radiation and may result in failure due to fatigue. When examining this, it is, however, not a practical course of action to carry out large scale strain measurement in pipeworks. Similarly, today it is not possible to make full scale FE models of the high frequency vibrations of complete pipe systems because of the overwhelmingly large models that are required. Therefore less demanding methods are needed for screening pipe systems to determine potential vibration noise and fatigue problems. This is equally important for design as for assessing existing pipeworks.

From an engineering point of view, a very attractive method to use for prediction of vibration is SEA [1–3]. This method is quick to apply and requires only general information about the structure investigated. For pipes it is natural to use the wave approach to SEA. The input data required are then, for each pipe element, the loss factor and the modal density and, for each coupling, the transmission factor. Also required are the input powers from the sources of vibration. Methods for calculating transmission factors in pipe–flange connections have been developed [4]. In the present work, simple expressions for the modal density in straight fluid filled pipes and the input power from mechanical and fluid point sources are derived. These expressions and those from reference [4] are then successfully used for statistical energy analysis of a simple pipe structure [5].

The analysis depends heavily on the work presented in two previous articles by the author [6, 7]. In reference [6] efficient routines for calculating the dispersion relations and

*Also at the Department of Vehicle Engineering, KTH, SE 100 44, Stockholm, Sweden.

0022–460X/97/500705 + 24 $25.00/0/sv971258

forced response in straight fluid filled pipes are developed. The pipe-wall motion is described by the Arnold and Warburton theory for thin walled cylinders [8] (the self-adjoint variant of the Love–Timoshenko shell theory [9]). The fluid motion is described by the Helmholtz equation and its radial dependence is approximated within cylindrical segments by FE polynomial shapefunctions. The resulting dispersion relations are compared with those found with the exact formulation by Fuller and Fahy [10], showing good agreement. The solutions of the equations of motion thus achieved are then used as base functions in a spectral finite element formulation. This method is a merger of the dynamic stiffness method and the finite element displacement method. Elements are formulated and assembled as in the standard FEM, while the trial functions are the local, frequency dependent, solutions of the equations of motion. In the present work, the routines presented in reference [6] are used to assess the accuracy of the approximate expressions developed for modal density and input power. To perform these comparisons, the spectral FE formulation for straight fluid filled pipes is here amended with expressions for forced response from fluid sources.

In reference [7] simplified equations of motion for the radial–axial vibrations of fluid filled pipes have been presented. The dynamic behaviour of a pipe is quite different for frequencies above and below the ring-frequency, this frequency occurring when the in-plane extensional wavelength in the pipe is equal to its circumference. Pipes for conveying fluids most often have diameters in the range 1 cm–1 m, so, for steel pipes the ring-frequency is in the range 160 kHz–1.6 kHz. Consequently, many noise and vibration problems are related to frequencies well below the ring-frequency. For such frequencies there is, for each trigonometric order, $n = 1, 2, 3, \ldots$, only one vibration mode that may propagate. Upon scrutinizing the cross-sectional mode shapes for the propagating modes, it is seen that they are almost as if inextensional: that is, almost without circumferential in-plane strain. By assuming this to be valid while restricting the analysis to lower frequencies, for which the axial wavelength is long compared to the cylinder radius and for which higher order fluid modes are cut off, the simplified theory is derived. It is found that the equations of motion for the radial–axial vibration of straight fluid filled pipes, for each trigonometric order, are equal to those for a Timoshenko beam on a Winkler foundation. This foundation stiffness describes the circumferential flexural stiffness of the pipe-wall. To make the present work self-contained, in section 2 there is a brief recapitulation of the simplified theory and the criteria for its application. A spectral FE formulation based on this theory is also presented and the application to forced response problems, in section 4, gives additional insight to the theory's potential and limitations.

In the present work, the equivalent beam theory is the basis for the derivation of modal density and input power in the propagating radial–axial waves. This means that the results do not apply when higher order fluid modes are cut on, nor for frequencies above half the ring-frequency. Also, the axisymmetric, $n = 0$, motion is not covered by the theory in reference [7] and is not accounted for in the present work. The dynamics of the axisymmetric modes are so different from that of the radial–axial modes considered in this paper that they deserve a special presentation.

Previously, Heckl was the first to calculate approximate formulas for the mode count and modal density in cylinders [11]. Most recently, Langley, using Donnell theory while neglecting the in-plane inertia, derived the modal density and mode count in cylindrical shells [12]. In both these works the circumferential wavenumber is treated as a continuous function of frequency. Often, pipes are very long and only a few circumferential modes can propagate. If so, there is a large increase in the mode count at those frequencies when an additional circumferential mode is cut on. The expressions derived in the present work account for this increase.

The modal density for fluid filled pipes has not previously been calculated. For vehicle-related problems, statistical energy analysis is often applied, with the cylindrical structure and the contained fluid treated as different subsystems, and thus having independent mode counts [13]. This is also the approach used for the analysis of high frequency vibrations of gas filled pipes [14]. For frequencies below cut-on of higher order fluid modes, however, the analysis in references [6, 7] suggests that the appropriate approach is to use "wet" modes: that is, to treat the fluid filled pipe as one structure. Perhaps, though, one should distinguish between waves of different trigonometric order, n, or between waves of "type 1" and "type 2" [12], (see section 3.2.1 below). By using the equivalent beam theory this may be accomplished.

The frequency-averaged point mobility of thin walled cylinders was calculated by Heckl [11]. Fuller [15] considered a fluid filled pipe using Donnell theory for the cylinder and an analytical description for the fluid reaction to cylinder motion. Fuller used the results in reference [10] to find the dispersion relations-requiring the solution of a non-linear eigenvalue problem- and then calculated the response in the pipe using complex integration theory. Because of the complexity of the mathematics used and the numerical difficulties that may occur when solving non-linear problems, the approach is primarily useful in a research situation. Möser *et al*. derived closed form approximations of the frequency average of the real part of the mobility [16]. They used a beam approximation below the cut-on of the $n = 2$ mode and Heckl's result [11] at higher frequencies while reducing the mobility accounting for the inertia of the fluid expressed as a function of n. In this inertia term, however, the frequency dependence of n is not clear. Also, the increase in modal density resulting from the increased inertia is not accounted for. As discussed above, Finnveden formulated spectral finite elements to be used for forced response analysis of fluid filled pipes [6]. In the present work, the results obtained by using this method are compared to those arrived at by using the beam theory presented in section 2. Also in the present work, frequency averages of the real part of the point mobility are calculated by using results from the equivalent beam theory. It is found that frequency band averages of the input power to a point-excited fluid filled pipe are calculated within a fraction of a second on a PC, with good accuracy.

To the author's knowledge, the only previous calculation of the high frequency response of a fluid filled pipe to fluid excitation was made by Fuller [17], using the same approach as in reference [15]. In the present work, the efficient spectral finite element formulation for pipes [6] is developed to handle fluid excitation. This excitation is also included as a generalized force in the equivalent beam theory. Comparisons are made showing that the modal mobility derived with the beam theory is very accurate at frequencies below and around a radial–axial mode cut-on frequency, while there are gross errors at even higher frequencies. The total point mobility, however, is predominantly governed by the modes that are near cut-on, and is therefore accurately calculated by the beam theory up to frequency limits given in section 2. Thus, as an example, for a water filled steel pipe with a diameter of 100 mm, the simple theory derived in this work is accurate for calculating the input power from mechanical and fluid point sources for frequencies up to approximately 3 kHz.

2. EQUIVALENT BEAM THEORY

2.1. SIMPLIFIED EQUATIONS OF MOTION FOR FLUID FILLED CYLINDERS

In reference [7] simplified equations describing the propagating radial–axial waves in fluid filled pipes were presented. As these equations form the basis of the work presented here, they are briefly reiterated.

In thin walled cylinder theory the equations of motion are formulated by using a Fourier decomposition of the circumferential dependence of the displacements and assuming plane stress in the cylinder cross-section according to the Kirchhoff hypothesis. The displacements are [6]

$$u_x = (u - z\,\partial w/\partial x)\cos(n\phi), \qquad u_\phi = (v + z(v + nw)/R)\sin(n\phi), \qquad u_z = w\cos(n\phi), \quad (1)$$

where R is the cylinder radius and where u, v and w are the displacements in the x, ϕ and z directions on the cross-sectional mid-plane; see Figure 1.

In reference [7] it was found that the circumferential in-plane motion, for propagating radial–axial waves $n = 1, 2, 3, \ldots$, is almost as if inextensional. Assuming this, $v = -w/n$. The analysis is then restricted to lower frequencies, for which the non-dimensional wavenumber (axial wavenumber times radius) is not large and for which higher order fluid modes are cut off. Thus, the motion of fluid filled pipes is given by

$$EI_n\,\partial^2\theta/\partial x^2 = GAK_n(\theta + \partial w/\partial x) - \rho\omega^2 I_n\theta,$$

$$GAK_n\left[\frac{\partial}{\partial x}\left(\theta + \frac{\partial w}{\partial x}\right) + C_n\frac{\partial^2 w}{\partial x^2}\right] = (K_w - \omega^2 M_e)w, \quad (2)$$

where stationary time dependence of the form $e^{-i\omega t}$ is assumed, where E is the Young's modulus, G is the shear modulus and ρ is the density, and where

$$\theta = n^2 u/R. \quad (3)$$

Also in equation (2), the cross-sectional area A, the equivalent area moment of inertia I_n, the equivalent shear factor K_n, the equivalent mass per unit length M_e, stiffness K_w and the factor C_n are given by

$$A = 2\pi T_c R, \qquad K_n = 1/(2n^2), \qquad I_n = I_y/n^4, \qquad I_y = \pi T_c R^3,$$

$$M_e = \rho A/2\left(1 + \frac{1}{n^2} + \frac{2\mu}{n}\right), \qquad K_w = \beta\frac{EA/2}{1 - \nu^2}\left(\frac{n^2 - 1}{R}\right)^2,$$

$$C_n = 2\beta(n - 1/n)^2/K_n. \quad (4)$$

Here T_c is the shell thickness, ν is the Poisson ratio and β and μ are non-dimensional numbers for the ratio of shell thickness to radius and for the ratio of fluid mass to shell mass:

$$\beta = T_c^2/12R^2, \qquad \mu = R\rho_f/2T_c\rho. \quad (5)$$

ρ_f is the fluid density.

In equation (2), the term proportional to C_n describes the restraint against twist of the pipe wall. For thin walled pipes, low order n, and/or low frequencies, this term may be

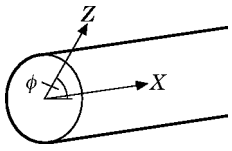

Figure 1. The cylinder co-ordinate system.

neglected. Equations (2) are then equal to those for a Timoshenko beam on a Winkler foundation having stiffness per unit length, K_w. This "foundation stiffness" describes the circumferential flexural stiffness of the pipe-wall.

For lower frequencies, equations (2) are simplified to be as those for an Euler beam on a Winkler foundation:

$$EI_n\,\partial^4 w/\partial x^4 + K_w w - \omega^2 M_e w = 0, \qquad \theta = -\partial w/\partial x. \tag{6}$$

Equations (2) and (6) also apply when losses proportional to either stiffness or inertia are present: that is, they apply equally when

$$E = E_0(1 - \mathrm{i}\eta_e), \qquad G = G_0(1 - \mathrm{i}\eta_s), \qquad \rho = \rho_0(1 + \mathrm{i}\eta_v), \qquad \rho_f = \rho_{f0}(1 + \mathrm{i}\eta_f). \tag{7}$$

2.1.1. *Wavenumbers*

When using the equivalent Timoshenko beam theory (2), the propagating wavenumbers, for the mode with circumferential non-dimensional wavenumber n, are given by

$$k_n R = [H + [\,][H^2 + M(Q - \Omega_1^2)]^{1/2}]^{1/2}, \tag{8}$$

where Ω_1 is

$$\Omega_1 = \omega R/\sqrt{E/\rho}, \tag{9}$$

and where

$$H = (M + \Omega_1^2 - QC_n/(1 + C_n))/2,$$

$$M = (\omega^2 M_e - K_w)R^2/(GAK_n(1 + C_n)),$$

$$Q = (GAK_n R^2)/(EI_n) = n^2 G/E. \tag{10}$$

The wavenumbers resulting from the application of the equivalent Euler beam theory, equation (6), are similarly given by

$$k_n R = R\left[\frac{\omega^2 M_e - K_w}{EI_n}\right]^{1/4} = n[\Omega_1^2(1 + 1/n^2 + 2\mu/n) - \beta(n^2 - 1)^2]^{1/4}. \tag{11}$$

Note, in accordance with the suggestion in reference [7], that the rod value of the axial rigidity is used and thus, for convenience, the parameter Ω_1 is introduced. From thin walled shell theory, upon assuming plane stress, it appears that the plate value should be used instead, this being a factor $1/\sqrt{1 - \nu^2}$ larger. While no theoretical justification for the decrease in stiffness has been found, it was concluded in reference [7] that the results obtained by using equations (8) and (11) will agree exactly with those found by using accurate thin walled cylinder theory when the frequency tends to zero. Thus, the previously reported error in the equivalent Euler beam theory [18] (dependent on the Poisson ratio) disappears.

The parameter Ω_1 is also found in reference [12]. Here, in the discussions and in the figures, however, the standard non-dimensional frequency parameter Ω will be used:

$$\Omega = \omega R/c_L, \qquad c_L^2 = E/\rho(1 - \nu^2), \qquad \Omega^2 = (1 - \nu^2)\Omega_1^2. \tag{12}$$

2.1.2 *Criteria for application*

In reference [7] the results of numerical experiments suggested that equations (2) are used with good accuracy when the non-dimensional axial wavenumber $k_n R$ is not larger than the non-dimensional circumferential wavenumber, n: that is, for frequencies

$$\Omega < 1/\sqrt{1 + 1/n^2 + 2\mu/n}. \tag{13}$$

Similarly, the Euler beam equation (6) applies for frequencies below a tenth of this.

Both equations (2) and (6) are valid only up to about half the cut-on frequencies for the higher order fluid modes. For $n = 1$, the most restrictive case, this limiting frequency is approximately given by

$$\Omega = (1{\cdot}8/2)c_f/c_L, \tag{14}$$

where c_f is the sound speed in the fluid.

Finally, for frequencies close to the ring-frequency, the assumption of inextensional circumferential in-plane motion is not valid. Hence, the equivalent beam theories are not likely to be valid above a third of, or perhaps half of, the ring-frequency.

2.2. SPECTRAL FINITE ELEMENT FORMULATION

In section 4, the forced response of pipes excited by mechanical point forces and fluid monopole sources are calculated. For the equivalent Timoshenko beam theory, this is done with the dynamic stiffness method developed in reference [19]. When using this method the functional, similar to the Lagrangian, which is stationary for true motion of the system is needed. Considering equations (2) shows that it is

$$L_p = \int \Bigg[EI_n \frac{\partial \theta^a}{\partial x}\frac{\partial \theta}{\partial x} + GAK_n\left(\theta^a + \frac{\partial w^a}{\partial x}\right)\left(\theta + \frac{\partial w}{\partial x}\right) + GAK_nC_n \frac{\partial w^a}{\partial x}\frac{\partial w}{\partial x} + (K_w - \omega^2 M_e)w^a w - \rho\omega^2 I_n \theta^a \theta \Bigg] \mathrm{d}x. \tag{15}$$

The superscript a denotes the complex conjugate of the displacements in an adjoint, negatively damped, system. Without losses this would be the complex conjugate of the displacements and, in this case, L_p would be the Lagrangian. The formulation for non-conservative motion when using an adjoint system was proposed in reference [20]. It has been used by Gladwell [21] and Morse and Ingard [22]. Its application to beam structures has been discussed in some detail in reference [19] and the application to fluid filled pipes has been demonstrated in reference [6].

The base functions, used in the spectral finite element formulation, are derived as the solutions of the equations of motion corresponding to the functional L_p: that is, the solutions of equations (2). When expressing these equations as a set of coupled first order ordinary differential equations, it is found that expanding in the derivatives of w results in numerical problems at lower frequencies, when the in-plane shear is negligible. Instead, the derivative of w is expressed as the difference between the "shear angle" and θ, so the following definitions are made:

$$m = \partial\theta/\partial x; \qquad \gamma = \theta + \partial w/\partial x. \tag{16}$$

These equations and those resulting when they are inserted into equations (2) are a set of four first order ordinary differential equations. Upon assuming solutions of these of the form $\exp(\alpha, x)$, a linear eigenvalue problem results which is solved by standard methods.

The base functions thus achieved are used as trial functions in a spectral finite element formulation for arbitrarily long pipes as in reference [19], or [6].

3. MODE COUNT AND MODAL DENSITIES

3.1. MODE COUNT

In uni-axial, prismatic, waveguide systems the resonances occur approximately when

$$kL = N\pi, \tag{17}$$

where k is a wavenumber in the direction of the waveguide, L is the length and N is any positive integer. The non-dimensional Helmholtz number, kL, is a measure of the size of the waveguide. The accuracy of the expression (17) depends on the boundary conditions. However, the magnitude of the error in the Helmholtz number is always less than $\pi/2$, so the relative error in equation (17) diminishes for large waveguides. For thin walled cylinders, equation (17) is exact if the boundary conditions are "simply supported": that is, if they are $\partial u/\partial x = v = w = \partial^2 w/\partial x^2 = 0$. Also for a fluid filled cylinder, equation (17) is exact, if the cylinder is simply supported and if the fluid obeys pressure release conditions, $p = 0$, at the pipe ends.

The mode count, $N_c = N_c(\omega)$, is the number of modes having resonance below the frequency ω. Consider a fluid filled pipe at frequencies below the cut-on of higher order fluid modes and below the cut-on of the $n = 1$ torsional mode at $\Omega \approx 0{\cdot}7$. At those frequencies, there is only one real solution of the dispersion relations for each $n \geqslant 1$. Hence, for simply supported and pressure release boundary conditions, if the mode count is considered as a continuous variable of the Helmholtz number, it is

$$N_c = 2/\pi \sum_{n=1}^{n_{max}} k_n(\omega)L, \tag{18}$$

where k_n is the wavenumber for the trigonometric order n and where the factor of two signifies that there are two modes of vibration in a cylinder having equal wavenumbers. The summation is for the modes with cut-on frequencies below the frequency considered. When using the equivalent beam theories (or the Flügge theory and neglecting terms of the order β^2 [23]) while assuming frequencies well below cut-on of higher order fluid modes, n_{max} is given by

$$n_{max} = \max(n)\colon \beta \frac{n^2(n^2-1)^2}{1+n^2+2n\mu} < \Omega^2. \tag{19}$$

For an *in-vacuo* cylinder, dimensional analysis shows that the non-dimensional wavenumber, $k_n R$, is a function of only n, v, β and Ω. The influence of the Poisson ratio on resonance frequencies is small [24], so the numerical examples below are restricted to $v = 0{\cdot}3$. The normalized mode count, N_n, is here defined as

$$N_n = T_c/LN_c. \tag{20}$$

Apart from the slight dependence on v, as n_{max} is determined by β and Ω, N_n is a function of only these two non-dimensional numbers.

Heckl calculated approximate formulas for the mode count and modal density in cylinders [11]. Langley, using Donnell theory while neglecting the in-plane inertia, derived the modal density and mode count in cylindrical shells [12]. For frequencies below the ring

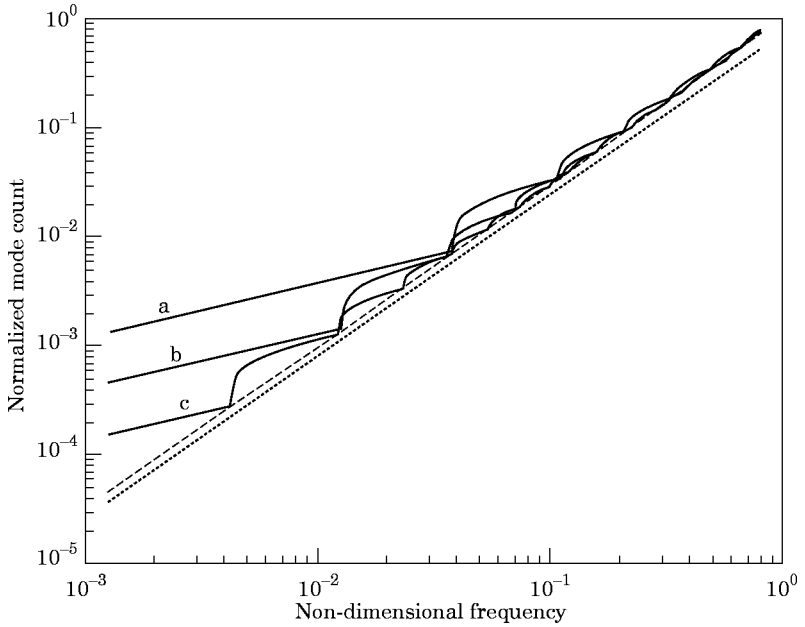

Figure 2. The normalized mode count in cylinders. · · · , Equation (21); ----, equation (22); ——, Arnold and Warburton theory; a, $T_c = R/20$; b, $T_c = R/60$; c, $T_c = R/180$.

frequency, the expressions for the normalized mode counts are [25, Table V.1] and [12, equations (10) plus (11)]

$$(N_n)_{Heckl} = 3\sqrt{3}\Omega^{3/2}/2\pi, \tag{21}$$

$$(N_n)_{Langley} = \sqrt{12(1-\nu^2)}/\pi \int_{\arccos\sqrt{\Omega_1}}^{\pi/2} [\Omega_1^2 - \cos^4\theta]^{1/2}\, \mathrm{d}\theta. \tag{22}$$

Notably, both these expressions for the normalized mode count are independent of β. The normalized mode counts according to Heckl and Langley are shown in Figure 2. Also shown are the exact (i.e., according to the Arnold and Warburton theory) results for cylinders with thickness $T_c = R/20$, $T_c = R/60$ and $T_c = R/180$. Besides being approximately 18% low, the results of Heckl agree with those of Langley at lower frequencies. As stated by both authors, for frequencies where only the beam mode is cut on, the results from equations (21) and (22) deviate largely from those achieved by using a more accurate cylinder theory. Both equations (21) and (22) are derived with the mode count considered as a continuous function of not only the axial Helmholtz number but also of the circumferential wavenumber. Thus, no account is taken of the increase of the mode count at the cut-on frequencies. In addition to this, equations (21) and (22) underestimate the average mode count at lower non-dimensional frequencies, most probably as the Donnell theory overestimates the cut-on frequencies for small n.

3.2. MODAL DENSITY FOR CYLINDERS

In SEA, the modal density is central. It is defined for a frequency band between frequencies ω_l and ω_u as

$$n_{dens} = \frac{N_c(\omega_u) - N_c(\omega_l)}{\omega_u - \omega_l}. \tag{23}$$

Often the limit $\omega_u \to \omega_l$ is taken, thus resulting in an expression valid not only in frequency bands but for a particular frequency. However, this expression is singular at cut-on if the mode count is based on equation (18).

The normalized modal density is here defined as

$$n_n = \frac{T_c c_L}{LR} n_{dens} = \frac{N_n(\Omega_u) - N_n(\Omega_l)}{\Omega_u - \Omega_l}, \tag{24}$$

which, if the mode count is as in equation (18), also may be written as

$$n_n = \frac{2}{\pi} \frac{T_c}{R} \sum_{n=1} \frac{k_n(\Omega_u)R - k_n(\Omega_l)R}{\Omega_u - \Omega_l}, \tag{25}$$

provided that the convention that $k_n(\omega) = 0$ if ω is below the cut-off frequency for mode n is adopted.

The normalized modal density is a function of only β, ν and Ω. It is calculated by using the mode count expression (22) and equation (24). It is also calculated by equation (25), in which case the wavenumbers are calculated with the Arnold and Warburton theory and with the equivalent Timoshenko beam theory, equation (8). For a cylinder with wall thickness $T_c = R/60$, in Figure 3 are shown swept one-third octave band averages of the normalized modal densities: that is, at each frequency is shown the third octave band average resulting when this frequency is the centre frequency in the band. The results confirm the conclusions drawn above. The Donnell theory underestimates the modal density for frequencies when kR is small, that is, for a pipe with $T_c = R/60$, for frequencies below a tenth of the ring frequency. The equivalent beam theory predicts the modal density accurately at frequencies below a third of the ring-frequency. Consequently, in contrast to the thin walled shell structures often found in vehicles, for pipe systems the modal

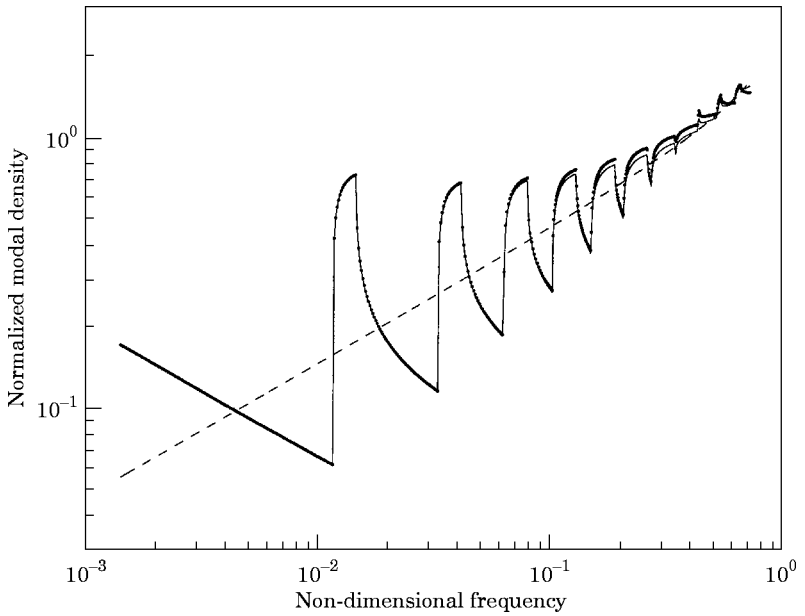

Figure 3. Swept one-third octave band averages of normalized modal density in a cylinder with thickness $T_c = R/60$. ——, Arnold and Warburton theory; · ·, equivalent Timoshenko beam; ----, derived from equation (22).

density is most easily found by using equation (25), with the wavenumbers calculated by equation (8) or (11).

3.2.1. *Type* 1 *and type* 2 *modes*

Langley distinguished between "type 1" waves, having motion restricted mainly by the flexural stiffness of the cylinder wall, and "type 2" waves having motion restricted mainly by in-plane stiffness [12]. The axial wavenumbers for type 1 waves decrease with increasing circumferential wavenumber—that is, with increasing n—whereas the opposite is true for type 2 waves. Langley classified these types according to the axial wavenumber's dependence on the circumferential wavenumber. That is, with the axial wavenumber considered to be a continuous function of n, waves with n larger than that given by $\partial k_n/\partial n = 0$ are considered as type 1. Perhaps some physical insight is given—certainly computational simplicity is gained—if they are classified according to which stiffness dominates. With reference to Figures 2 and 3 in reference [7] and to equation (6), a vibrational mode is type 1 at cut-on where the circumferential flexural stiffness dominates. At somewhat higher frequencies, the cross-sectional bending—that is, axial in-plane stiffness—becomes the most important term and the wave is of type 2. For the inextensional motion considered here, the restraints against motion from these two terms are equal when the wavenumber is such that $K_w = EI_n k_n^4$. Near cut-on, the Euler beam approximation for the wavenumbers is accurate. By using this, the criterion is found to be such that at cut-on and up to $\sqrt{2}$ times this frequency a wave is type 1 whereas for even higher frequencies it is type 2.

3.3. MODAL DENSITY FOR FLUID FILLED PIPES

The modal density for fluid filled pipes has not previously been calculated. Dimensional analysis shows that the normalized mode count is a function of β, ν, Ω, c_f/c_L and μ. Below half the cut-on frequency of higher order fluid modes, the wavenumbers are independent of c_f/c_L, there is only one propagating wave for each $n \geqslant 1$ and the equivalent beam theories apply up to frequency limits given in section 2.1.2. Thus, the modal density for fluid filled pipes is found from equation (25), using the wavenumbers given either by equation (8) or (11). The normalized modal densities for water filled steel pipes with wall thickness $T_c = R/20$ and $T_c = R/180$ have been calculated, and in Figure 4 are shown results obtained with the beam theories and with the routines in reference [6]. It is seen that the beam theories predict the modal density accurately for frequencies well above those given in section 2.1.2.

3.3.1 *Approximate modal density*

The beam theories efficiently provide good estimates of the modal densities. In many situations it is, however, beneficial to have simple closed form expressions, explicitly showing the parameter dependence. To that end the results by Langley [12] are modified to account approximately for fluid loading.

By using the Donnell theory while neglecting the in-plane inertia, the dispersion relations for cylinders have been simplified in reference [12], to become

$$\Omega_1^2 = G = G(kR, n, \beta, \nu), \tag{26}$$

where the explicit expression for G is given in equation (1) of reference [12]. Similarly, if the fluid loading is included as in the derivation of the equivalent beam theories (by increasing the cylinders radial inertia), the dispersion relation is

$$(1 + 2\mu/n)\Omega_1^2 = G. \tag{27}$$

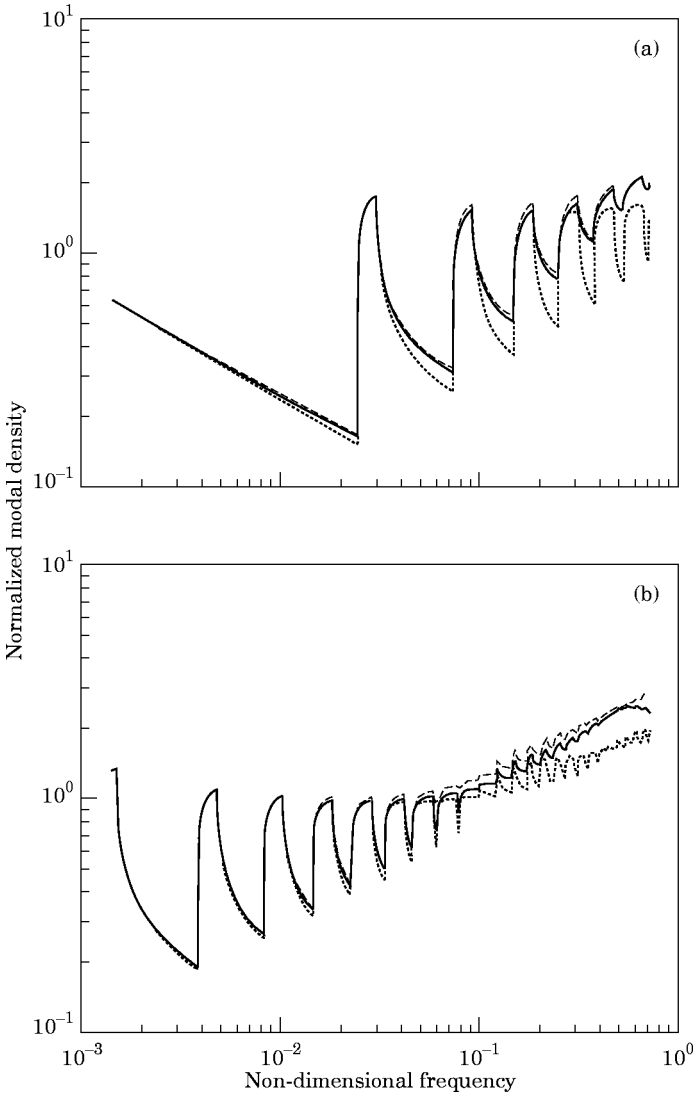

Figure 4. (a) The swept one-third octave band averaged normalized modal density in a water filled steel pipe, $T_c = R/20$. ——, Arnold and Warburton theory; · · ·, equivalent Euler beam; ---, equivalent Timoshenko beam. (b) As (a), but $T_c = R/180$.

The modal density, expressing the increase of the mode count, is largely determined by the modes with large n, being just above cut-on. From the Donnell theory, the cut-on frequencies are

$$\Omega_{cut\text{-}on}^2 = \frac{\beta n^4}{1 + 1/n^2 + 2\mu/n}. \tag{28}$$

The fluid loading terms in equations (27) and (28) are important only if $2\mu/n > 1$. Upon assuming this, those n that are close to cut-on are approximately expressed as $n \approx (2\mu\Omega^2/\beta)^{1/5}$. Inserting this expression into the left side of equation (27) yields the dispersion relation as in equation (26), but with a different scaling of the frequency:

$$(1 + 2\mu(2\mu\Omega^2/\beta)^{-1/5})\Omega_1^2 = G. \tag{29}$$

The analysis by Langley may now be employed to find the mode count. If the slight frequency dependence of the fluid loading is neglected when the derivative of the mode count with respect to frequency is taken, then the modal density is also calculated as in reference [12]. Applying this yields the normalized modal density as

$$n_n = \frac{T_c c_L}{LR} n_{dens} = F_l \sqrt{6F_l\Omega_1}/\pi \mathrm{K}(0{\cdot}5 + F_l\Omega_1/2), \tag{30}$$

$$F_l = \sqrt{1 + 2\mu(2\mu\Omega^2/\beta)^{-1/5}}, \tag{31}$$

where K is the complete elliptic integral of the first kind. With an error that is less than 0·5% for frequencies $F_l\Omega_1 < 0{\cdot}3$, a linear curve fit is used to approximate the elliptic integral. The normalized modal density is then approximated as

$$n_n = F_l \sqrt{6F_l\Omega_1}/\pi(1{\cdot}85 + F_l\Omega_1/2). \tag{32}$$

The modal density has been calculated in octave bands by using this expression and equation (25), in which case the wavenumbers are found by the accurate routines in reference [6]. In Figure 5 the results are presented for water filled steel pipes with wall thickness $T_c = R/20$ and $T_c = R/180$. It is seen that for frequencies from around the cut-on of the $n = 2$ mode up to approximately a third of the ring frequency, the approximation (32) is quite accurate, on the average.

4. INPUT POWER FROM SIMPLE SOURCES

4.1. MECHANICAL POINT SOURCE

Consider an infinite fluid filled pipe excited by a point force, at $x = x_0$, $\phi = 0$, having magnitude f_0 in the radial direction. When using the equivalent Timoshenko beam

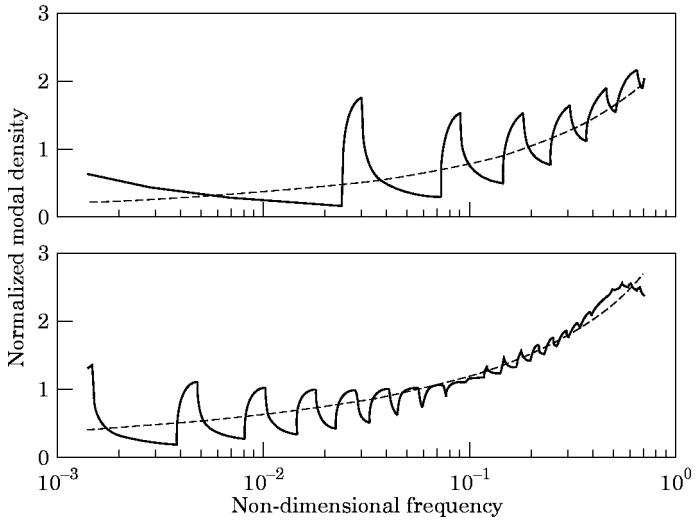

Figure 5. The swept one-third octave band averaged normalized modal density in a water filled steel pipe, upper, $T_c = R/20$; lower, $T_c = R/180$. ——, Arnold and Warburton theory; ---, equation (32).

TABLE 1

Geometrical and material parameters

Young's modulus, E (N/m^2)	Density of steel, ρ (kg/m^3)	Density of water, ρ_f (kg/m^3)	Sound velocity of water, c_f (m/s)
210×10^9	7800	1000	1500

	$R/T_c = 20$	$R/T_c = 60$	$R/T_c = 180$
Wall thickness, T_c (mm)	7·5	2·5	0·8333 . . .

Loss factors, $\eta_e = \eta_s = \eta_v = \eta_f = 0{\cdot}01$; cylinder radius, $R = 0{\cdot}15$ m.

theory, the equations of motion, for each n, are as in equations (8) but with a right hand side:

$$EI_n\,\partial^2\theta/\partial x^2 - GAK_n(\theta + \partial w/\partial x) + \rho\omega^2 I_n\theta = 0,$$

$$GAK_n\left[\frac{\partial}{\partial x}\left(\theta + \frac{\partial w}{\partial x}\right) + C_n\frac{\partial^2 w}{\partial x^2}\right] - (K_w - \omega^2 M_e)w = -f_0\delta(x_0 - x). \tag{33}$$

These equations have been solved by the spectral finite element presented in section 2.2, for comparison of the results with those calculated by using the routines in reference [6]. The calculations were made for a water filled steel pipe with wall thickness $T_c = R/60$; the data are shown in Table 1. The magnitudes and phases of the point mobilities for the $n = 1$ and $n = 3$ modes are shown in Figures 6 and 7. At lower non-dimensional frequencies the results are in excellent agreement. For the $n = 1$, beam mode, the result deviates largely from around the limiting frequency for the equivalent Euler beam theory. For the $n = 3$ mode, the arguments of the mobilities start to deviate almost immediately after cut-on

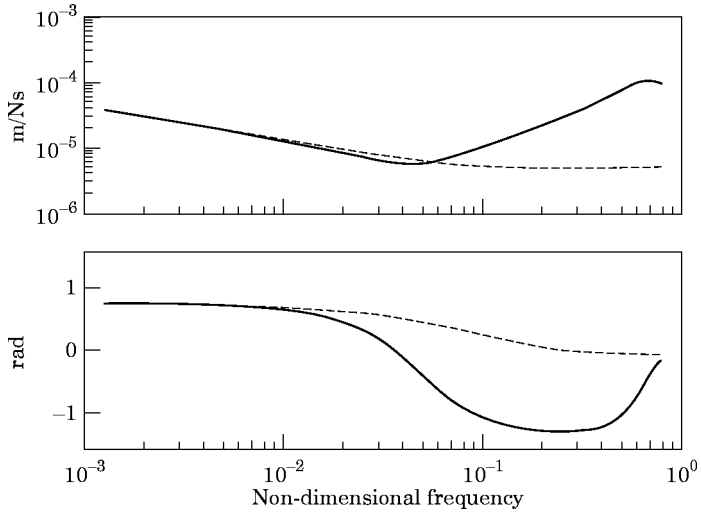

Figure 6. The point mobility for the $n = 1$ mode in a water filled steel pipe, $T_c = R/60$: upper, magnitude; lower, argument. ——, Arnold and Warburton theory; ----, equivalent Timoshenko beam.

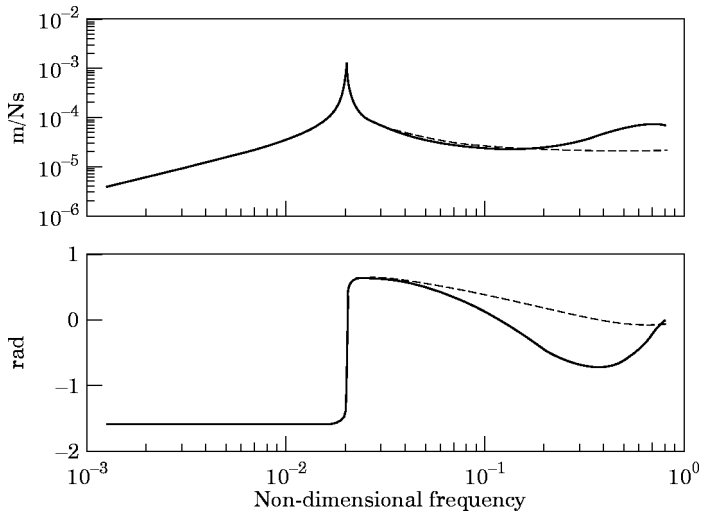

Figure 7. As Figure 6, but $n = 3$.

whereas the magnitudes are approximately equal up until the limits given in section 2.1.2. The beam theory predicts the reactive part of the mobility to be of mass character while the cylinder theory at higher frequencies predicts a stiffness character, most probably caused by the flexibility of the higher order non-propagating evanescent modes. The displacements of these modes are neglected in the beam theory.

Another source of error for the beam theory arises from the approximation of the radial dependence of the fluid velocity potential (equation (43) of section 4.2.2), resulting in a frequency independent fluid modal mass. The propagating radial–axial modes are subsonic; for these modes the fluid radial wavenumber is imaginary having roughly the same magnitude as the axial wavenumber. This means that the exact solution for the fluid motion is a modified Bessel function of the first kind with an argument that is small at cut-on, then increasing with increasing frequency (see reference [10]). Thus, well above cut-on the fluid velocity will decrease (approximately) exponentially away from the pipe-wall. As frequency increases, the rate of decay increases and less fluid takes part in the motion, so the fluid inertia for the propagating modes will decrease.

The total point mobility has been calculated with the beam theory and the routines in reference [6]. The results are compared in Figure 8, showing an excellent agreement up to a third of the ring frequency. At this frequency there are nine waves which are cut-on, and as the calculations were made considering $n = 1, 2, \ldots, 25$, the approach with the routines in [6] requires quite extensive calculations. When using the beam theory, however, the results for 2000 frequency points are found within a few minutes on a PC.

To sum up, the equivalent Timoshenko beam theory predicts the point mobility for a cross-sectional mode accurately below and around its cut-on frequency. For frequencies well above the cut-on the restraints on motion imposed in the derivation of the equivalent beam theory are apparently too restrictive. Thus, at high frequencies the magnitude of a cross-sectional mode's mobility is underestimated and the phase is in gross error. The total point mobility, however, is predominantly given by the mobility of those modes that are near cut-on. For these modes the equivalent Timoshenko beam theory applies. Consequently, up to the frequency limits given in section 2.1.2, the total point mobility is accurately calculated by the beam theory.

4.1.1. *Input power*

To determine the input power from the point force, only the real part of the input mobility is needed. The frequency average of this function is found by employing the mode of analysis in section v.4.c of reference [25]:

$$\mathrm{Re}(Y) = \sum_{n=1}^{n_{max}} \frac{\pi/2}{L[2M_e + |\theta_n/w_n|^2 2\rho I_n]} \frac{N_c(\omega_u) - N_c(\omega_l)}{\omega_u - \omega_l}. \tag{34}$$

Here, n_{max} is found either from equation (19) or, perhaps more conveniently, by just calculating the wavenumbers for increasing n, stopping when no propagating mode is found. The factor of two in the inertia terms accounts for the fact that the mass per unit area in the pipe is twice M_e. In equation (34), θ_n and w_n are elements of the eigenvector for the propagating mode with trigonometric dependence n. These eigenvectors may be

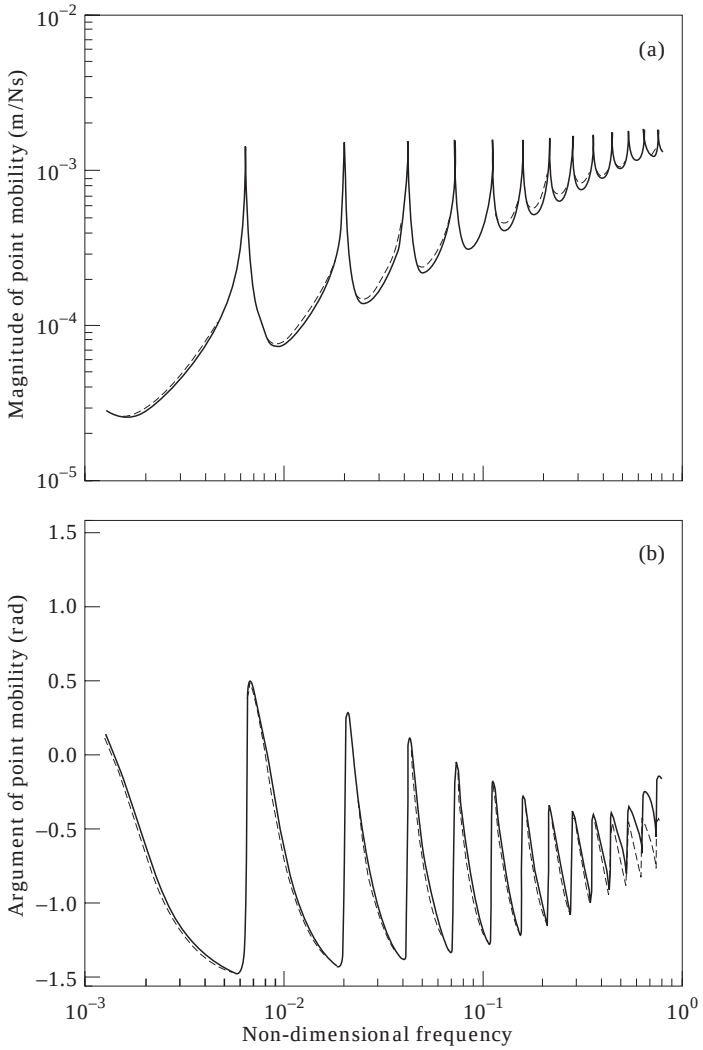

Figure 8. (a) Magnitude of point mobility in a water filled steel pipe, $T_c = R/60$; ——, Arnold and Warburton theory; ----, equivalent Timoshenko beam. (b), As (a) but argument of mobility.

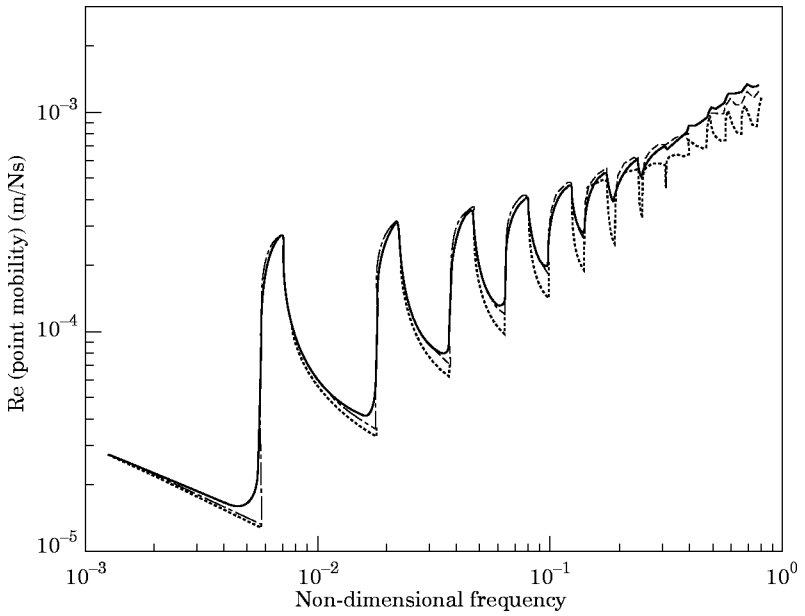

Figure 9. the swept one-third octave band averages of the real part of the point mobility in a water filled steel pipe, $T_c = R/60$. ——, Arnold and Warburton theory; ----, equivalent Timoshenko beam; · · ·, equivalent Euler beam.

found from the homogenous version of equation (33). If, instead, the Euler beam approximation of the pipe is considered, then $\theta_n = -\mathrm{i}k_n w_n$. This approximation gives an overestimation of the axial in-plane inertia at higher frequencies. Near cut-on, however, where a mode's contribution to the real part of the mobility is largest, the errors are small. By using this approximation, equation (34) is simplified to become

$$\mathrm{Re}(Y) = \frac{1}{\rho c_L A} \sum_{n=1} \frac{1}{(1 + 1/n^2 + 2\mu/n + (k_n R/n^2)^2)} \frac{k_n(\Omega_u)R - k_n(\Omega_l)R}{\Omega_u - \Omega_l}, \tag{35}$$

where A is the cross-sectional area and where the summation extends over those n for which there is a propagating mode. The wavenumbers may be found from either equation (8) or (11), or with a more accurate theory. When using any of the equivalent beam theories, this expression could be evaluated within a fraction of a second in a PC. In Figure 9 the one-third octave band averages of this function are compared to the results given by using the spectral FE formulation in reference [6]. The results from the equivalent Euler beam theory are good near the cut-on frequencies where the point mobility is governed by type 1 modes [12] while, well above cut-on, where the type 2 modes are important, the input power is underestimated. The spectral FE calculations were made for a quite "lossy" pipe, see Table 1. This explains why there are increases in the real part of the point mobility just below cut-on. By modifying equation (35) using the approach in a recent article by Langley this small discrepancy may be avoided [26]. Besides this, results from equation (35), with wavenumbers calculated by equation (8), deviate from results obtained by using accurate thin walled cylinder theory by no more than ± 1 dB. It is seen that for calculation of frequency averaged input power, both beam theories may be used with good accuracy up to the frequency limits given in section 2.1.2.

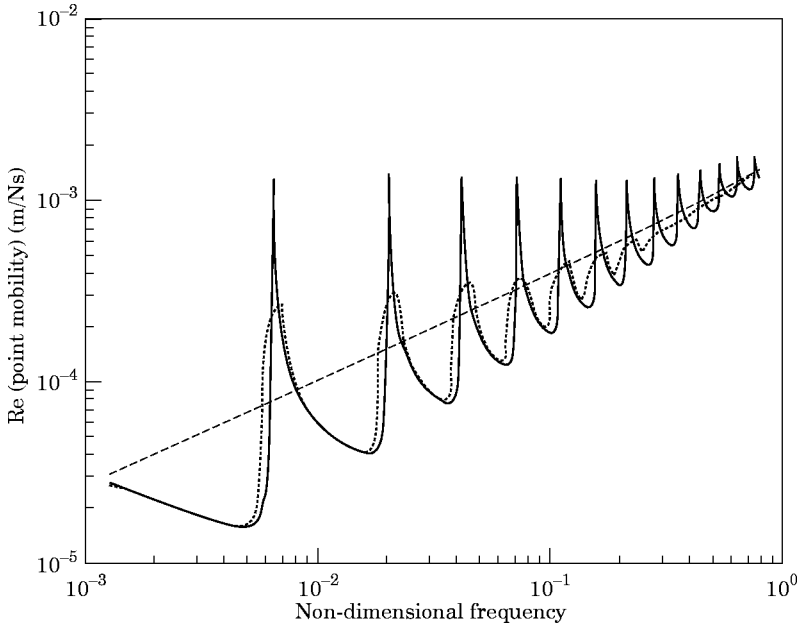

Figure 10. The real part of the point mobility in a water filled steel pipe $T_c = R/60$. ——, Arnold and Warburton theory; · · ·, swept one-third octave band averages; ----, equation (36).

4.1.2. *Approximate expression for input power*

By employing the mode of analysis in section 3.3.1, the expression for the point mobility could be even further simplified. That is, in equation (35) the in-plane inertia of the cylinder is entirely neglected and the n-dependence of the fluid loading is approximated as in equation (29). Upon doing this, the real part of the point mobility and the input power from the point force are found to be given by

$$\mathrm{Re}(Y) = n_n/(4\rho c_L T_c^2 F_l^2), \qquad P_{in} = |f_0|^2\,\mathrm{Re}(Y), \tag{36}$$

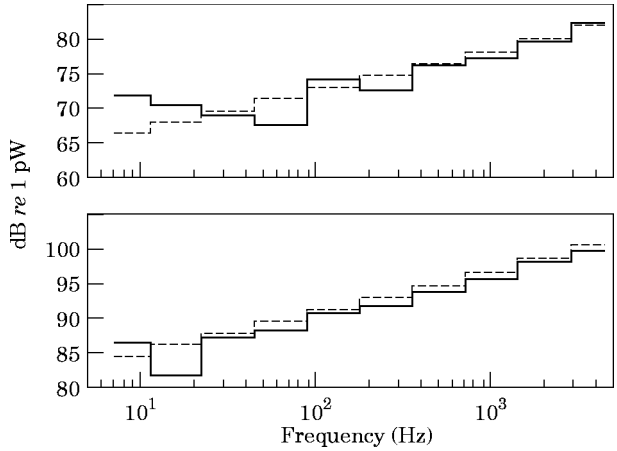

Figure 11. The octave band averaged input power in water filled steel pipes from a point force with unit amplitude; upper, $T_c = R/20$; lower, $T_c = R/180$. ——, Arnold and Warburton theory; ----, equation (36).

where the normalized modal density, n_n, is defined in equation (24) and is calculated as in equation (32). The approximation of the relative contribution to the inertia from fluid loading, F_l, is given in equation (31). Notably, the fluid loading increases the modal density by a factor $(F_l)^{3/2}$ while the level of the mobility is decreased by the fluid inertia: that is, by a factor F_1^2. To some extent, these two effects cancel each other.

In Figures 10 and 11 the results given by using the approximate formula (36) are compared to the results given by using the accurate thin walled cylinder theory. It is seen that, once the $n = 2$ shell mode is cut-on, equation (36) is accurate enough for prediction

4.2. POWER INPUT FROM FLUID MONOPOLE SOURCE

4.2.1. *Monopole excitation*

Consider a monopole source, within the fluid in the pipe. For a lossless fluid, if this source were in free field, the equation of motion would be [22, equation (7.1.14)]

$$\nabla^2 p + (\omega/c_f)^2 p = -q_0 \delta(r), \tag{37a}$$

and the resulting sound pressure, p, at distance r from the source is

$$p(r) = \frac{q_0}{4\pi r} \mathrm{e}^{\mathrm{i}\omega(r/c_f - t)}. \tag{37b}$$

With such a source in a pipe, the functional L [6, equation (28)] describing the motion of a fluid filled pipe is adjusted to be $L = L_{cyl} - L_F - B_{fc}$, where

$$L_F = L_f + \int \left[\frac{(\psi^a q_0 + \psi q_0)}{\omega(1 + \mathrm{i}\eta_f)} \frac{\delta(x - x_0)\delta(r - r_0)}{r} \right] \mathrm{d}x\, r\, \mathrm{d}r. \tag{38}$$

Here the functionals L_{cyl} and L_f describe the homogenous vibrations of the cylinder and the fluid, B_{fc} describes the coupling and ψ is an analogue to the fluid velocity potential and is given by

$$p = \rho_f \omega \cos(n\phi)\psi. \tag{39}$$

In equation (69) of reference [6] a trial function for ψ in a pipe element of length $2L$ is assumed:

$$\psi(x, r) = \mathbf{g} * \mathbf{B_f} * \mathbf{B_F} * \mathrm{diag}\,(\exp(\boldsymbol{\alpha} x - \boldsymbol{\alpha_p} L)) * \mathbf{A} * [\mathbf{V_1}^{\mathrm{T}} \quad \mathbf{V_2}^{\mathrm{T}}]^{\mathrm{T}},$$
$$\mathbf{g}(r) = [(r/R) \quad (r/R)^2 \quad \cdots \quad (r/R)^{N_f}], \tag{40}$$

where N_f is the number of d.o.f. used to describe the radial dependence of the fluid motion and where the matrices $\mathbf{B_f}$ and $\mathbf{B_F}$ and the vectors $\boldsymbol{\alpha}$ and $\boldsymbol{\alpha_p}$ are as defined in reference [6]. The vectors $\mathbf{V_1}$ and $\mathbf{V_2}$ contain the cylinder nodal displacements and the fluid nodal d.o.f., $\boldsymbol{\Psi_1}$ and $\boldsymbol{\Psi_2}$, at the ends of the pipe at $x = -L$ and $x = L$. The matrix $\mathbf{A}$ is defined in equation (72) of reference [6] so that at the pipe ends

$$\psi(-L, r) = \mathbf{g}(r) * \boldsymbol{\Psi_1}, \qquad \psi(L, r) = \mathbf{g}(r) * \boldsymbol{\Psi_2}. \tag{41}$$

Consequently, having a node at $x = x_0$, upon inserting the trial function (40) into the functional L_F it becomes

$$L_F = L_f + \frac{q_0}{\omega(1 + \mathrm{i}\eta_f)} * \mathbf{g}(r_0) * [\boldsymbol{\Psi}(x_0) + \boldsymbol{\Psi}^a(x_0)]. \tag{42}$$

Thus, the monopole excitation could be directly included as a generalized force vector in the routines in reference [6].

4.2.2. *Monopole excitation of the equivalent beam elements*

When using the equivalent beam theories presented in section 2, the trial function for the fluid sound pressure is, as in reference [7],

$$p = \rho_f \omega \cos(n\phi)\psi, \qquad \psi = f(x) r^n. \tag{43}$$

From equations (26) and (27) of reference [7], and upon neglecting the fluid compressibility and axial inertia, L_F and B_{fc} are

$$L_F = L_f + \frac{q_0 r_0^n}{\omega(1 + \mathrm{i}\eta_f)} (f + f^a)\delta(x - x_0),$$

$$L_f = -\frac{\pi \rho_f}{1 + \mathrm{i}\eta_f} R^{2n} \int [n f^a f] \, \mathrm{d}x,$$

$$B_{fc} = \pi \omega \rho_f R^{n+1} \int [f^a w + f w^a] \, \mathrm{d}x. \tag{44}$$

The functional $L = L_{cyl} - L_F - B_{fc}$ is stationary for the true motion. Only the latter two functionals depend on the fluid motion and, upon taking the variation of f^a, it is possible to solve for f:

$$f = \frac{(1 + \mathrm{i}\eta_f)\omega}{n R^{n-1}} w + \frac{(r_0/R)^n}{\pi \rho_f \omega R^n} \frac{q_0}{n} \delta(x - x_0). \tag{45}$$

Now, the variations of w^a and θ^a in L_{cyl} are taken and the value of f above is inserted into the resulting equations. The equations of motion for the equivalent Timoshenko beam are then found to be equation (33a) and

$$GAK_n \frac{\partial}{\partial x}\left(\theta + \frac{\partial w}{\partial x}\right) - (K_w - \omega^2 M_e) w = -\left(\frac{r_0}{r}\right)^n \frac{R q_0}{n} \delta(x - x_0). \tag{46}$$

Consequently (see equation (33)), the monopole source acts as a point force on the equivalent beam with magnitude

$$f_0 = (r_0/R)^n R q_0 / n. \tag{47}$$

The radial response of the pipe to a monopole source at $r_0 = 3R/4$ has been calculated by using the spectral finite element formulation for the equivalent Timoshenko beam and the routines in reference [6] with the excitation as in equation (42). The calculations were made for $n = 1, 2, \ldots, 25$. In Figures 12(a) and 12(b) are shown the magnitude and phase of the transfer mobility $-\mathrm{i}\omega w/q_0$ for a water filled steel pipe with wall thickness $T_c = R/60$. In Figure 13 is shown the overestimation of velocity level resulting from using the beam theory for pipes with wall thickness $T_c = R/20$ and $T_c = R/180$. At low frequencies and around the cut-on frequencies, the results are in good agreement. The beam theory overestimates the transfer mobility somewhat, most probably because the fluid is assumed to be incompressible. Even so, up to the frequency limits given in section 2.1.2, the errors (in narrow bands) are only 2 dB for the thick walled pipe and even less for the thin walled pipe.

4.2.3. *Input power*

When using the equivalent beam theories, the monopole source acts as an equivalent mechanical point source with magnitude as given in equation (47). This equivalent force

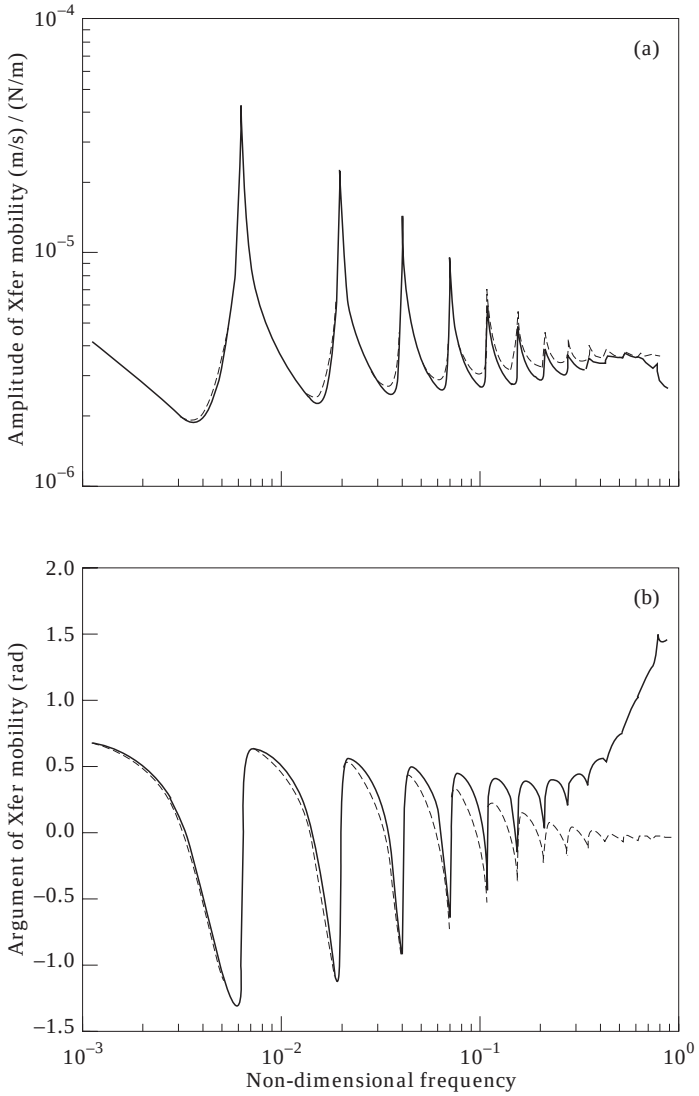

Figure 12. (a) The magnitude of the transfer mobility; monopole at $r = 3R/4$ to radial velocity of pipe-wall, $T_c = R/60$. ——, Arnold and Warburton theory; ----, equivalent Timoshenko beam. (b) As (a) but the argument of the mobility.

is a function of n and it is therefore difficult to find simple expressions for the input power, such as for a mechanical point force, equation (36). Equation (35), however, may be used to find frequency averages of input power. Another approach, valid also for narrow band calculation, is to use the spectral finite element formulation, presented in section 2.2. In this case, the input power, with the $n = 0$ modes disregarded, is given by

$$P_{in} = \sum_{n=1} \mathrm{Re}\,(f_0(n)(-\mathrm{i}\omega w_n)^*), \tag{48}$$

where w_n is the resulting radial displacement for the trigonometric order n and where f_0 is given in equation (47). Similarly, when using the routines in reference [6], it should be

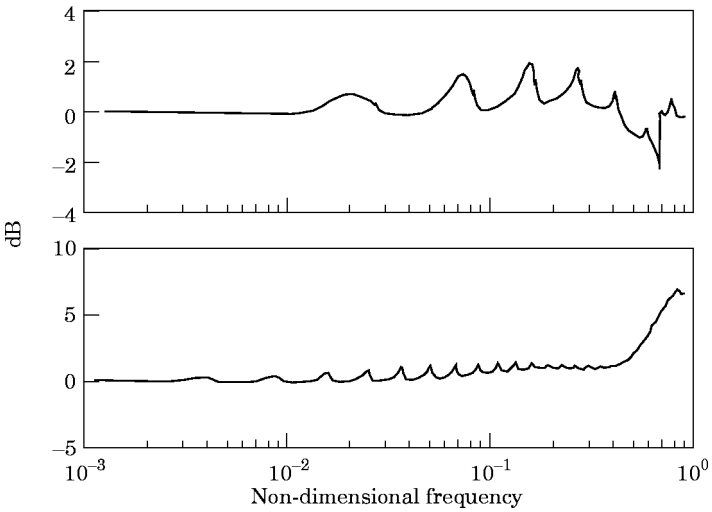

Figure 13. The error in velocity level of radial pipe vibrations excited by a fluid monopole source at $r = 3R/4$. Overestimation of the equivalent Timoshenko beam theory compared to Arnold and Warburton theory. Upper, $T_c = R/20$: lower, $T_c = R/180$.

possible to calculate the input power from the generalized force vector defined by equation (42) and the generalized nodal displacements $\mathbf{\Psi}$. A more independent calculation, however, results from considering the energy flow away from the source. The input power is then, by symmetry, calculated as twice the axial energy flow in the pipe. The intensity in thin walled cylindrical shells was calculated by Langley, using the Arnold and Warburton theory [9]. This result and the standard expression for the intensity in a fluid described by Helmholtz equation are used to formulate the energy flow in fluid filled pipes.

In Figure 14 are shown the input power in the modes $n = 1, 2, \ldots 8$ for a water filled steel pipe with wall thickness $T_c = R/20$. As for the mechanical point source, the input power is accurately calculated by the beam theory for frequencies around cut-on. Below

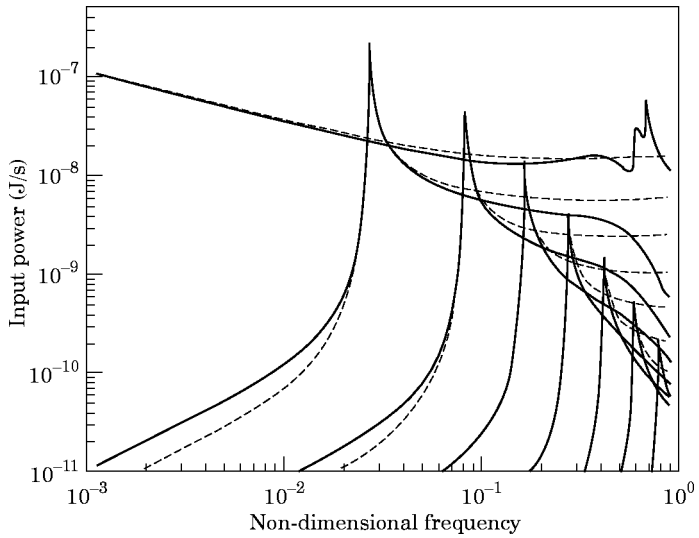

Figure 14. The input power from a fluid monopole source at $r = 3R/4$ in modes $n = 1, 2, \ldots, 8$; $T_c = R/20$. ——, Arnold and Warburton theory; ----, equivalent Timoshenko beam.

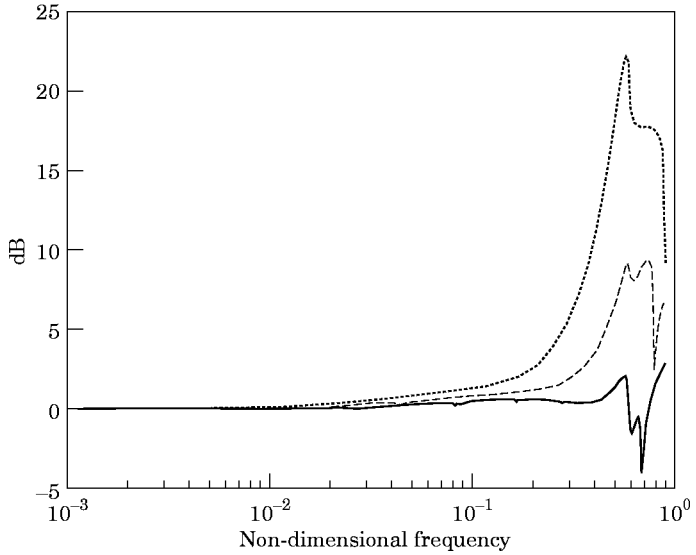

Figure 15. The error in the input power level from a fluid monopole source at $r = 3R/4$. Overestimation of the equivalent Timoshenko beam theory compared to Arnold and Warburton theory. ——, $T_c = R/20$; ----, $T_c = R/60$; · · · , $T_c = R/180$.

the cut-on frequencies there are only evanescent modes in the pipe which, if there is damping, may accept a small amount of input power. Most of these modes are neglected by the beam theory, this probably explaining the (quite irrelevant) underestimation of the input power for frequencies well below cut-on. At frequencies well above cut-on, the equivalent beam theory greatly overestimates the input power. Most probably, this is caused by errors in the assumed frequency independent shape function for the fluid motion, equation (43). As discussed in section 4.1, the accurate solution for the fluid velocity potential of the propagating modes is a modified Bessel function of the first kind. This function has, when the wavenumber is large, an approximately exponential decay away from the pipe-wall. The rate of this decay increases as frequency increases and thus the modal amplitude of the fluid–monopole source strength decreases. This behaviour of the accurate solution is not captured by the beam theory.

The total input power is predominantly given by the $n = 1$ beam mode and by those modes that are near cut-on. In Figure 15 are shown the errors in narrow bands of the sum of the input power in the modes $n = 1, 2, \ldots, 25$, for water filled steel pipes with wall thickness $T_c = R/20$, $T_c = R/60$ and $T_c = R/180$. As can be seen, the errors are very small up to the limits given in section 2.1.2.

5. CONCLUSIONS

Simple expressions for the modal density of straight fluid filled pipes and for the input power from mechanical and fluid point sources have been derived. The derivations are based on the simplified equations of motion for fluid filled pipes originally presented in reference [7]. In section 2 these equations were recapitulated and criteria for their application were given. The accuracy of the resulting expressions for modal density and input power were verified by the spectral FE method presented in reference [6]. Explicit

calculations were made for water filled steel pipes, and the analysis in reference [7] indicates that the results also apply for fluid filled pipes made of other materials.

The vibrational motion of pipes was described by using a Fourier decomposition of the circumferential dependence. The axisymmetric, $n = 0$, modes were not considered here. For each of the other trigonometric orders $n = 1, 2, \ldots$, there are at lower frequencies (below half the ring-frequency and below the cut-on frequencies for higher order fluid modes) only one radial–axial mode that may propagate. It is the modal density of these modes that has been considered. Two approximations were derived. One simple formula was derived from Langley's expression for empty cylinders [10] by including the inertia of the fluid as in the equivalent beam theories. The other approximation was derived on a waveguide basis, with the modal density for each trigonometric order being considered individually. In this case, each order is a one-dimensional system for which the modal density is found from the wavenumbers of propagating waves. By using this approximation, account is taken of the increase of the modal density around cut-on frequencies. It is also possible to identify the modal density of different trigonometric orders and of modes being of "type 1" and "type 2" [10]. Within the frequency limits of the simplified beam theory (as given in section 2.1.2) the accuracy of the closed form expression is comparable to those previously reported for *in-vacuo* cylinders [9, 10]. The more accurate waveguide expression is almost exact when compared to one-third octave band averages of the modal density calculated by using accurate thin walled cylinder theory and Helmholtz equation for the fluid.

A spectral FE formulation for the equivalent beam theory was presented. By using this, the mechanical point mobility was calculated and compared to the results from reference [6]. For each trigonometric order, the results show good agreement below and around its cut-on frequency. At even higher frequencies, the magnitude of the point mobility is underestimated and the phase is in gross error. Possible causes for these discrepancies are the neglect of the flexibility in the evanescent higher order structural modes and the overestimation of the fluid inertia. The total point mobility is predominantly given by the modes that are near cut-on. These modes are accurately modelled by the equivalent beam theory and, consequently, the total point mobility shows very good accuracy.

Frequency averaged input power from a mechanical point source was, as in reference [25], calculated as a function of the modal mass and modal density. By using the Euler beam approximation of the mode shapes and the Timoshenko beam approximation of the modal density, the input power was calculated in one-third octave bands with an error that is less than 1 dB. Alternatively, neglecting the in-plane inertia of the cylinder and using the closed form expression for the modal density results in a very neat formula. By using this formula, for frequencies above the cut-on frequency of the $n = 2$ mode and below half the ring frequency, the input power was estimated in octave bands with an error that is no more than 3 dB.

Monopole excitation was included here in the spectral FE formulation in reference [6] as a generalized force vector. It was also included in the equivalent Timoshenko beam formulation as an equivalent force on the beam. Comparing these formulations shows, as for the mechanical point force, good agreement below and around the cut-on frequencies. At frequencies well above cut-on, the discrepancies are, however, larger in this case. This is most probably because the beam theory does not account for the change at higher frequencies of the fluid mode shapes, and thus not for the change of the value of the generalized force. For a monopole at $r = 3R/4$, the total input power for all trigonometric orders was calculated with the equivalent beam theory and the routines from reference [6]. Up to the frequency limits given for the beam theory, the results agree to within 1 dB in narrow bands.

ACKNOWLEDGMENT

The financial support of TFR, Sweden, and EPSRC, U.K., is gratefully acknowledged.

REFERENCES

1. F. J. Fahy 1994 *Transactions of the Royal Society of London*, *Series A* **346**, 431–447. Statistical energy analysis: a critical overview.
2. R. H. Lyon and R. G. DeJong 1995 *Theory and Application of SEA*. London: Butterworth–Heinemann.
3. R. J. M. Craik 1996 *Sound Transmission through Buildings Using Statistical Energy Analysis*. Aldershot: Gower.
4. S. Finnveden 1997 *Proceedings of the 6th International Conference on Recent Advances in Structural Dynamics*, *Southampton*, 613–627. Vibration energy transmission in fluid-filled pipes connected with flanges.
5. S. Finnveden 1997 *Proceedings of the IUTAM Symposium on Statistical Energy Analysis*, *Southampton*. Statistical energy analysis of fluid-filled pipes (will be published by Kluwer academic publishers).
6. S. Finnveden 1996 *Journal of Sound and Vibration* **199**, 125–154. Spectral finite element analysis of vibration of straight fluid-filled pipes with flanges.
7. S. Finnveden 1997 *Journal of Sound and Vibration* **208,** 685–703. Simplified equations of motion for the radial–axial vibrations of fluid filled pipes.
8. R. N. Arnold and G. B. Warburton 1949 *Proceedings of the Royal Society of London*, *Series A* **197**, 238–256. Flexural vibrations of the walls of thin cylindrical shells having freely supported ends.
9. R. S. Langley 1994 *Journal of Sound and Vibration* **169**, 29–42. Wave motion and energy flow in cylindrical shells.
10. C. R. Fuller and F. J. Fahy 1982 *Journal of Sound and Vibration* **81**, 501–518. Characteristics of wave propagation in cylindrical elastic shells filled with fluid.
11. M. Heckl 1962 *Journal of the Acoustical Society of America* **34**, 1553–1557. Vibrations of point-driven cylindrical shells.
12. R. S. Langley 1994 *Journal of Sound and Vibration* **169**, 43–53. The modal density and mode count of thin cylinders and curved panels.
13. F. J. Fahy *Journal of Sound and Vibration* **13**, 171–194. Response of a cylinder to random sound in the contained fluid.
14. M. P. Norton and A. Pruiti 1991 *Applied Acoustics* **33**, 313–336. Universal prediction schemes for estimating flow-induced industrial pipeline noise and vibration.
15. C. R. Fuller 1983 *Journal of Sound and Vibration* **87**, 409–427. The input mobility of an infinite circular cylindrical elastic shell with fluid.
16. M. Möser, M. Heckl and K. H. Ginters 1986 *Acustica* **60**, 34–44. Zur schallausbreitung in flüssigkeitsgefüllten kreiszylindrishen rohren.
17. C. R. Fuller 1984 *Journal of Sound and Vibration* **96**, 101–110. Monopole excitation of vibrations in an infinite cylindrical elastic shell filled with fluid.
18. G. Pavic 1992 *Journal of Sound and Vibration* **154**, 411–429. Vibroacoustical energy flow through straight fluid filled pipes.
19. S. Finnveden 1994 *Acta Acustica* **2**, 461–482. Exact spectral finite element analysis of stationary vibrations in a rail way car structure.
20. P. M. Morse and H. Feshbach 1953 *Methods of Theoretical Physics*. New York: McGraw-Hill.
21. G. M. L. Gladwell 1966 *Journal of Sound and Vibration* **4**, 172–186. A variational formulation for damped acousto-structural problems.
22. P. M. Morse and K. U. Ingard 1968 *Theoretical Acoustics*. New York: McGraw-Hill.
23. G. Pavic 1990 *Journal of Sound and Vibration* **142**, 293–310. Vibrational energy flow in elastic cylindrical shells.
24. A. W. Leissa 1973 *Vibrations of shells* (NASA SP-288). Washington, D.C.: U.S. Government Printing Office.
25. L. Cremer, M. Heckl and E. E. Ungar 1988 *Structure-borne Sound*. Berlin: Springer-Verlag; second edition.
26. R. S. Langley 1994 *Journal of Sound and Vibration* **181**, 657–672. On the power input to point loaded hysteretically damped structures.